SPC 407
Supersonic & Hypersonic Fluid Dynamics

Lecture 9

December 18, 2016

Hypersonic Flow

Hypersonic flows have, up to the present, mainly been associated with the reentry of orbiting and other high altitude bodies into the atmosphere. For example, a typical Mach
number with altitude variation for a reentering satellite is **Mach 26**. When the Apollo spacecraft returned from the moon. it entered the atmosphere at Mach 36. These very high Mach numbers are associated with the extreme, high-Mach-number portion of the fight spectrum which is labeled as hypersonic
flight.

Hypersonic Flow
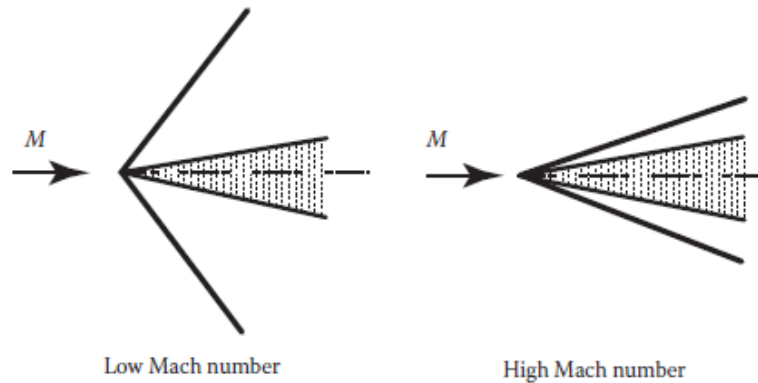
FIGURE 11.4
Shock angle at low and high supersonic Mach number flow over a wedge.
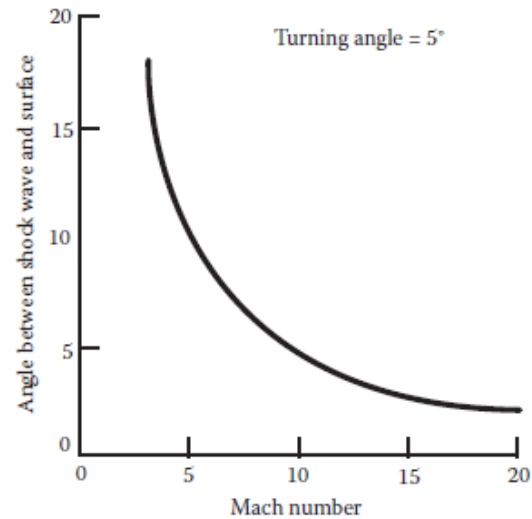
High-Temperature Flows

Assumptions that were used till now in this course are
- The specific heats of the gas are constant
- The perfect gas law, $p/\rho = RT$, applies
- There are no changes in the physical nature of the gas in the flow
- The gas is in thermodynamic equilibrium

However, if the temperature in the flow becomes very high, it is possible that some of these assumptions will cease to be valid.

https://www.youtube.com/watch?v=wNesL9CBlWk
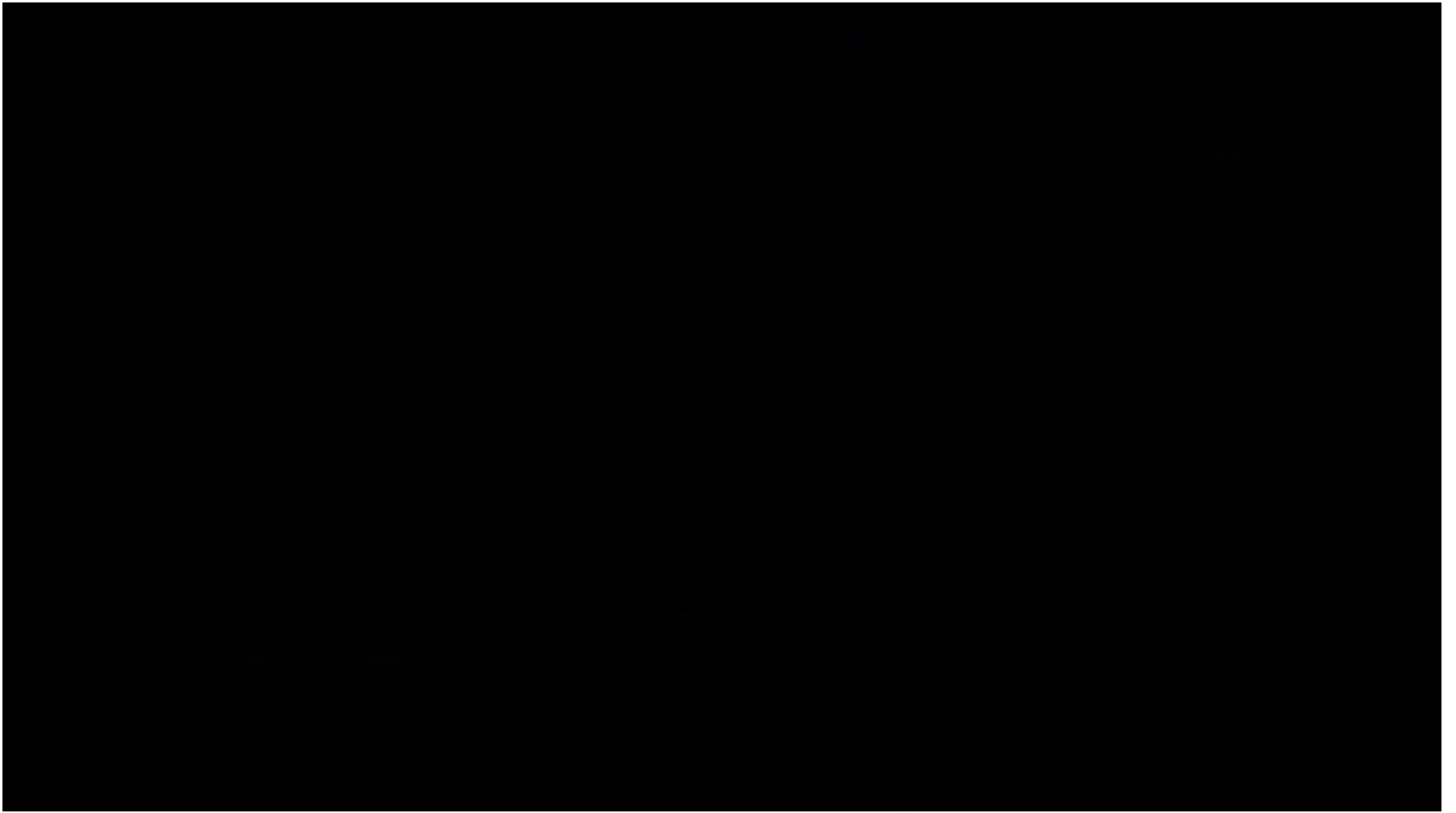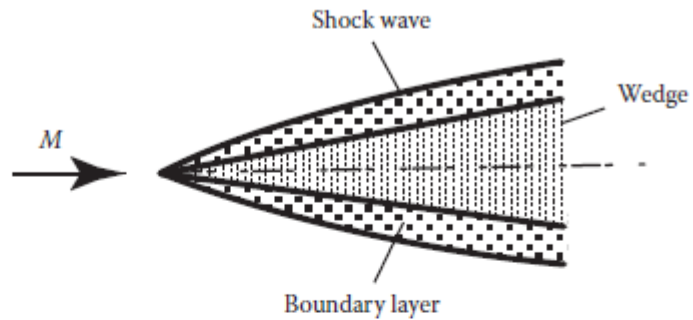
Hypersonic Flow

FIGURE 11.6
Interaction between shock wave and boundary layer in hypersonic flow over a wedge.
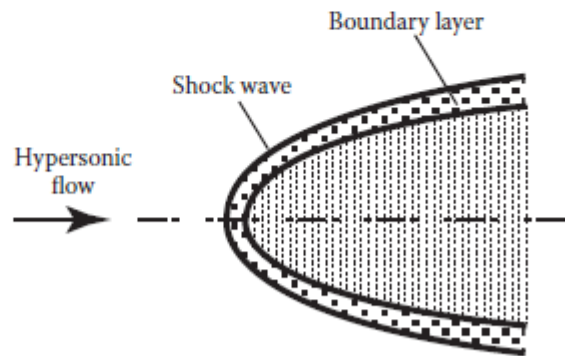
FIGURE 11.7
Interaction between shock wave and boundary layer in hypersonic flow over a curved body.

Hypersonic Flow
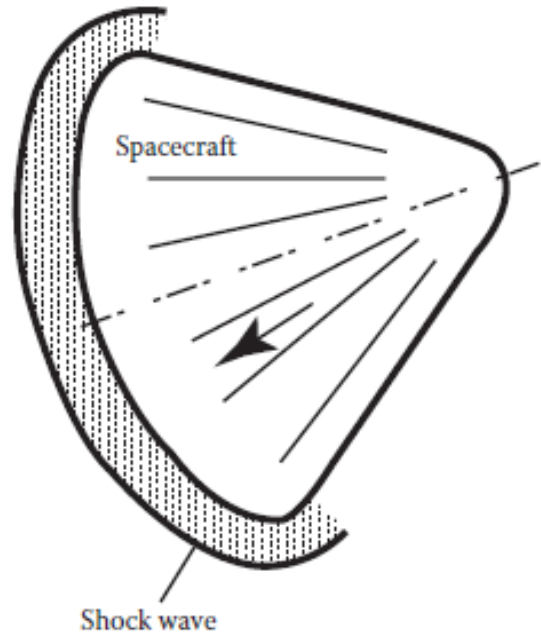
FIGURE 11.9
Flow over early spacecraft during reentry.

Hypersonic Flow

Physical Phenomena associated with Hypersonic Flows:
- Thin Shock Layer
- Viscous Interaction and Shock Layer Interaction with boundary layer
- High Temperarture Flows

Thin Shock Layer

Recall from oblique shock that, for a given flow deflection angle, the density increase across the shock wave becomes progressively larger as the Mach number is increased. At higher density, the mass flow behind the shock can more easily "squeeze through" smaller areas. For flow over a hypersonic body, this means that the distance between the body and the shock wave can be small. The flowfield between the shock wave and the body is defined as the shock layer, and for hypersonic speeds this shock layer can be quite thin.

Thin Shock Layer

For example, consider the Mach 36 flow of a calorically perfect gas with a ratio of specific heats = 1.4, over a wedge of 15 deg half-angle. From standard oblique shock theory
the shock wave angle will be only 18 deg as shown in Fig.
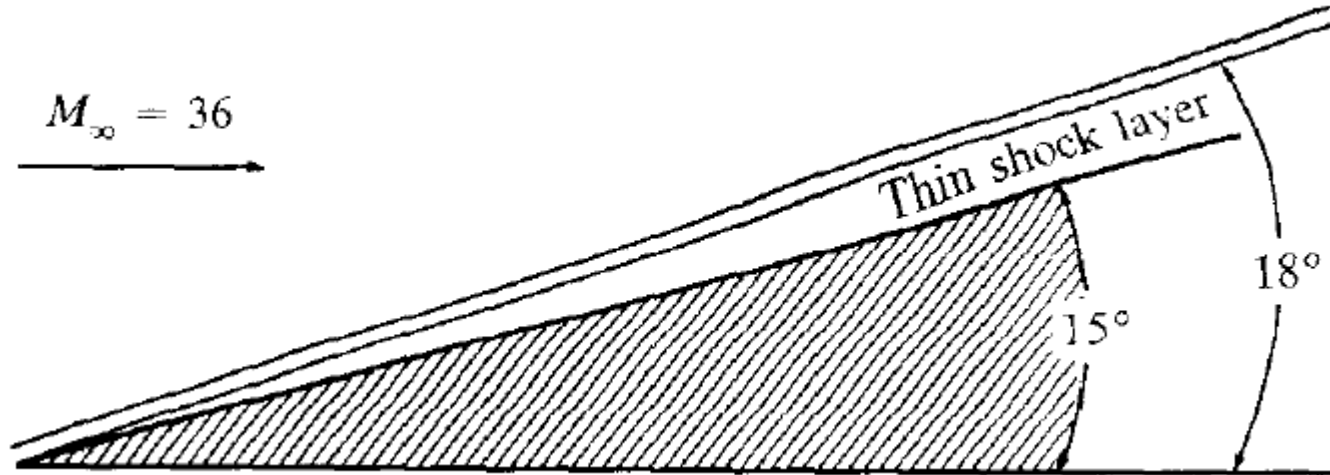
Viscous Interaction

Consider a boundary layer on a flat plate in a hypersonic flow, as sketched in Fig. A high-velocity, hypersonic flow contains a large amount of kinetic energy; when this flow is slowed by viscous effects within the boundary layer, the lost kinetic energy is transformed (in part) into internal energy of the gas-this is called viscous dissipation. In turn, the temperature increases within the boundary layer; a typical temperature profile within the boundary layer is also sketched in Fig. The characteristics of hypersonic boundary layers are dominated by such temperature increases.
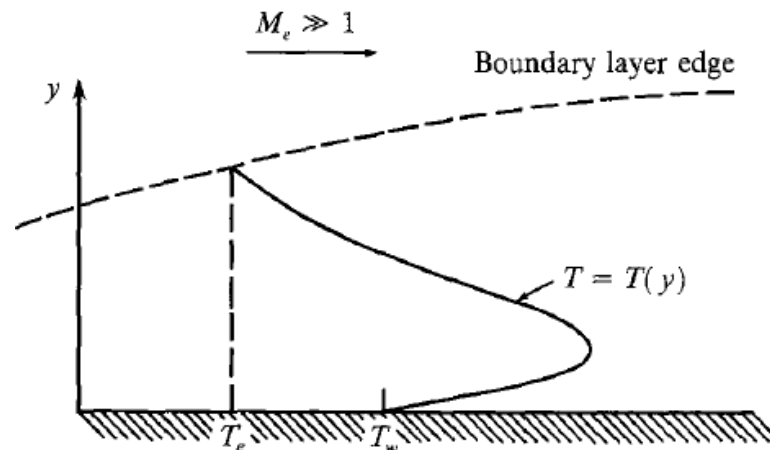
Viscous Interaction

The flat plate compressible laminar boundary layer thickness δ grows essentially as

$$\delta = \frac{M_\infty^2}{\sqrt{Re_x}}$$

where M_∞, is the free-stream Mach number, and Re_x, is the local Reynolds number. Clearly, since δ varies as the square of M_∞, it can become inordinately large at hypersonic speeds.

The thick boundary layer in hypersonic flow can exert a major displacement effect on the inviscid flow outside the boundary layer, causing a given body shape to appear much thicker than it really is. The major interaction between the boundary layer and the outer inviscid flow is called viscous interaction.

Viscous interactions can have important effects on the surface pressure distribution. hence lift, drag, and stability on hypersonic vehicles. Moreover, skin friction and heat transfer are increased by viscous interaction.

High Temperature Flow

The kinetic energy of a high-speed, hypersonic flow is dissipated by the influence of friction within a boundary layer. The extreme viscous dissipation that occurs within hypersonic boundary layers can create very high temperatures-high enough to excite vibrational energy internally within molecules, and to cause dissociation and even ionization within the gas.

High-temperature chemically reacting flows can have an influence on lift, drag, and moments on a hypersonic vehicle.

However, by far the most dominant aspect of high temperatures in hypersonics is the resultant high heat-transfer rates to the surface. Aerodynamic heating dominates the design of all hypersonic machinery, whether it be a flight vehicle, a ramjet engine to power such a vehicle, or a wind tunnel to test the vehicle. This aerodynamic heating takes the form of heat transfer from the hot boundary layer to the cooler surface.

High Temperature Flow

Conventional relationships for a normal shock wave at Mach 36 give

$$\frac{T_2}{T_1} = 253$$

However, at 59 km in atmosphere
T_1 = 258 K (i.e., −15°C)

Hence, the conventional normal
shock wave relations give the
temperature behind the
shock wave as

T_2 = 258 × 253 = 65,200 K

Shock
wave

$M = 36$

T_1 | T_2
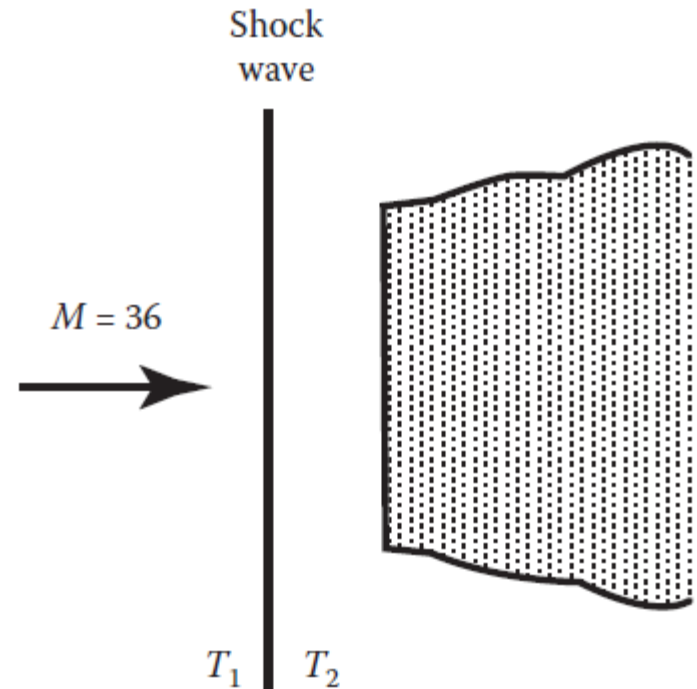
High Temperature Flow

At temperatures as high as these a number of so-called high temperature gas effects will become important. For example, the values of the specific heats, c_p and c_v, and their ratio, γ, change at higher temperatures, their values depending on temperature. For example, the variation of γ of nitrogen with temperature is shown in Figure. It will be seen from this figure that changes in γ may have to be considered at temperatures above about 500°C.
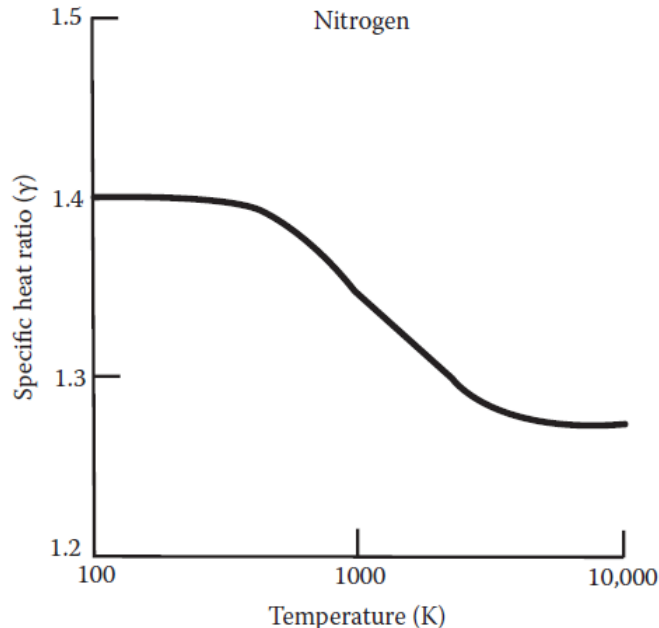
High Temperature Flow

Another high-temperature effect arises from the fact that, at ambient conditions, air is made up mainly of nitrogen and oxygen in their diatomic form. At high temperatures, these diatomic gases tend to dissociate into their monoatomic form, and at still higher temperatures, ionization of these monoatomic atoms tends to occur. Dissociation occurs under the following circumstances:
For 2000 K < T < 4000 K: $O_2 \rightarrow 2O$, i.e., the oxygen molecules break down to O molecules
For 4000 K < T < 9000 K: $N_2 \rightarrow 2N$, i.e., the nitrogen molecules break down to N molecules.

When such dissociation occurs, energy is "absorbed."

High Temperature Flow

Similarly, ionization occurs under the following circumstances:
For T > 9000 K

$$O \rightarrow O^+ + e^-$$

$$N \rightarrow N^+ + e^-$$

When ionization occurs, energy is again "absorbed."
Other chemical changes can also occur at high temperatures, e.g., there can be a reaction between the nitrogen and the oxygen to form nitrous oxides at high temperatures. This and the other effects mentioned above are illustrated by the results given in Figure

High Temperature Flow
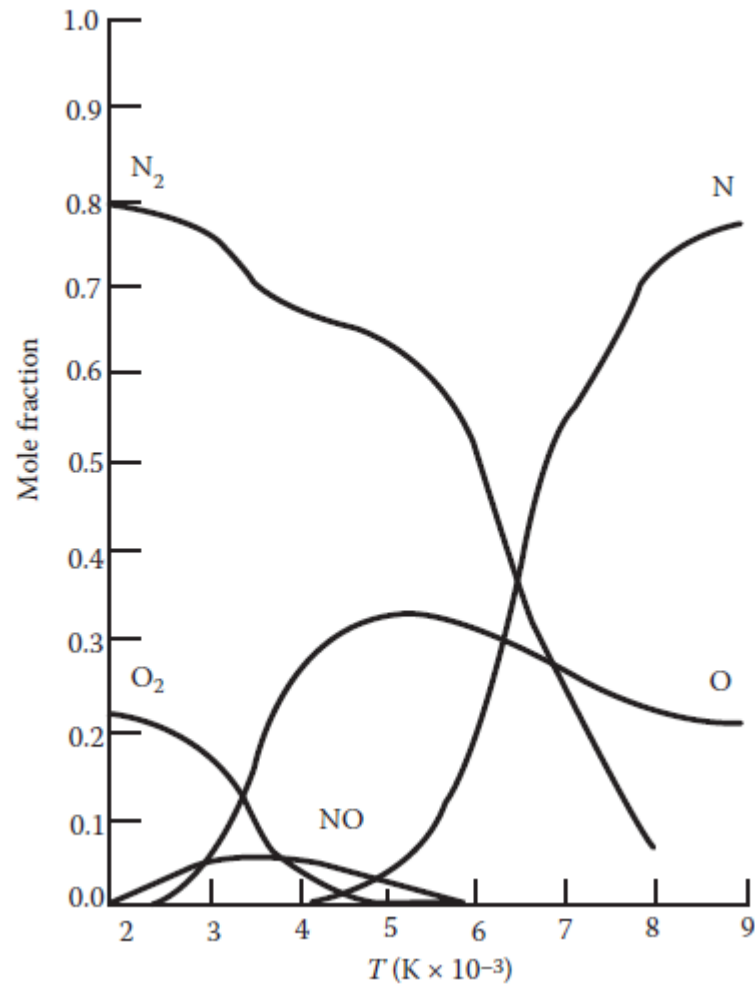
High Temperature Flow

Last figure shows the variation of the composition of air with temperature. It will be seen therefore that at high Mach numbers, the temperature rise across a normal shock may be high enough to cause specific heat changes and dissociation, and at very high Mach numbers, ionization. As a result of these processes, conventional shock relations do not apply.

For example, for the case discussed above, of a normal shock wave at Mach 36 at an altitude of 59 km in the atmosphere, as a result of these high temperature gas effects the actual temperature behind the shock wave is approximately

$$T_2 \approx 11,000 \text{ K}$$

rather than the value of 65,200 K indicated by the normal shock relations for a perfect gas.

HYPERSONIC SHOCK WAVE RELATIONS

The basic oblique shock relations was derived as the following

$$h_{01} = h_{02} \quad \rightarrow \quad T_{01} = T_{02}$$

$$Ma_{2,n} = \sqrt{\frac{(k-1)Ma_{1,n}^2 + 2}{2kMa_{1,n}^2 - k + 1}}$$

$$\frac{P_2}{P_1} = \frac{2k\,Ma_{1,n}^2 - k + 1}{k+1}$$

$$\frac{\rho_2}{\rho_1} = \frac{V_{1,n}}{V_{2,n}} = \frac{(k+1)Ma_{1,n}^2}{2 + (k-1)Ma_{1,n}^2}$$

$$\frac{T_2}{T_1} = [2 + (k-1)Ma_{1,n}^2]\frac{2k\,Ma_{1,n}^2 - k + 1}{(k+1)^2 Ma_{1,n}^2}$$

$$\frac{P_{02}}{P_{01}} = \left[\frac{(k+1)Ma_{1,n}^2}{2 + (k-1)Ma_{1,n}^2}\right]^{k/(k-1)} \left[\frac{(k+1)}{2k\,Ma_{1,n}^2 - k + 1}\right]^{1/(k-1)}$$

HYPERSONIC SHOCK WAVE RELATIONS

The basic oblique shock relations was derived as the following

The θ-β-Ma relationship:

$$\tan \theta = \frac{2 \cot \beta (Ma_1^2 \sin^2 \beta - 1)}{Ma_1^2(k + \cos 2\beta) + 2}$$
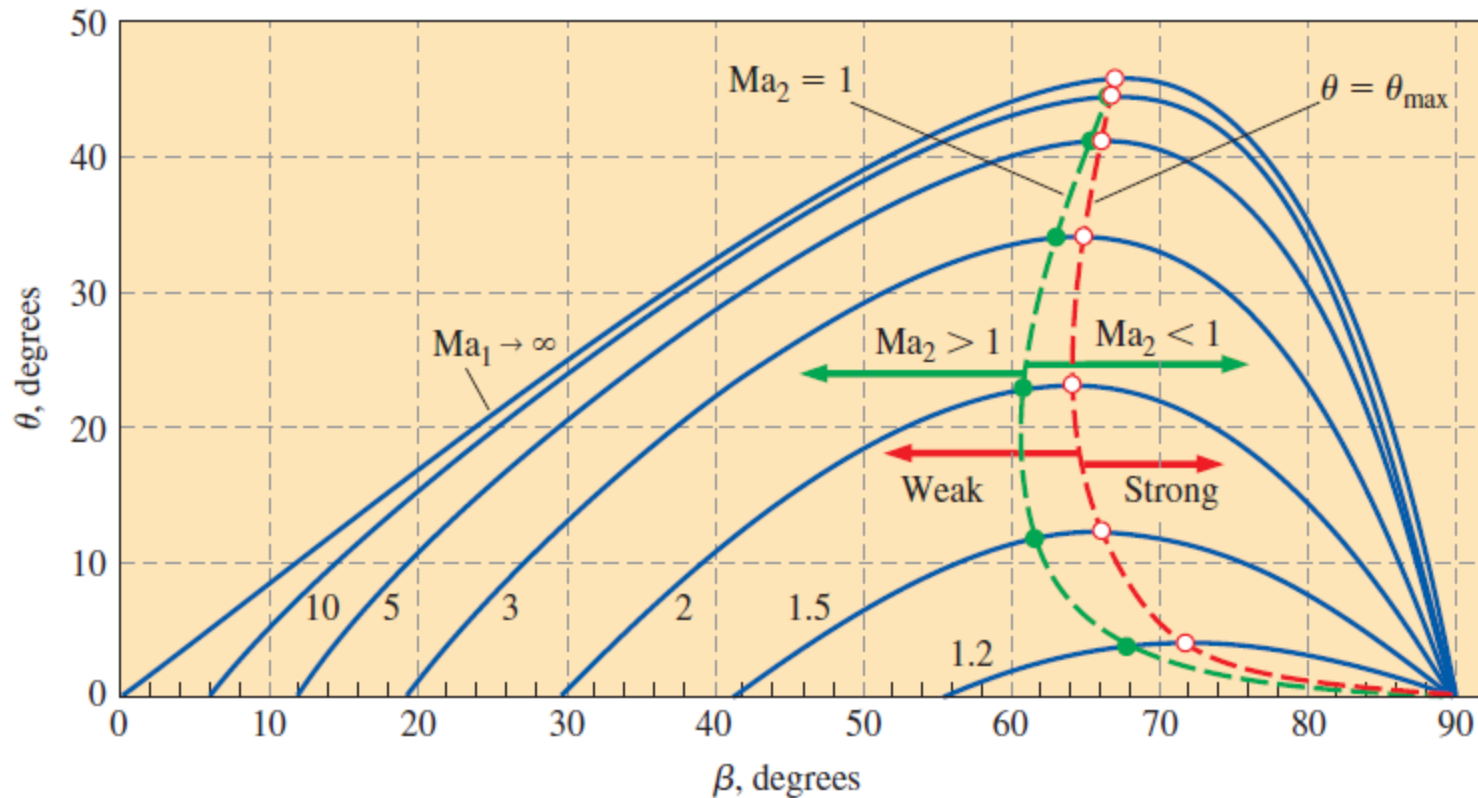
HYPERSONIC SHOCK WAVE RELATIONS

Consider the flow through a straight oblique shock wave, as sketched in Figure. Upstream and downstream conditions are denoted by subscripts 1 and 2, respectively.

For pressure ratio across the wave is given by

Exact:
$$\frac{p_2}{p_1} = 1 + \frac{2\gamma}{\gamma + 1}\left(M_1^2 \sin^2 \beta - 1\right)$$

where β is the wave angle. In the limit as M_1 goes to infinity, the term $M_1 \sin^2 \beta \gg 1$, and hence Eq. becomes

as $M_1 \rightarrow \infty$:
$$\boxed{\frac{p_2}{p_1} = \frac{2\gamma}{\gamma + 1} M_1^2 \sin^2 \beta}$$
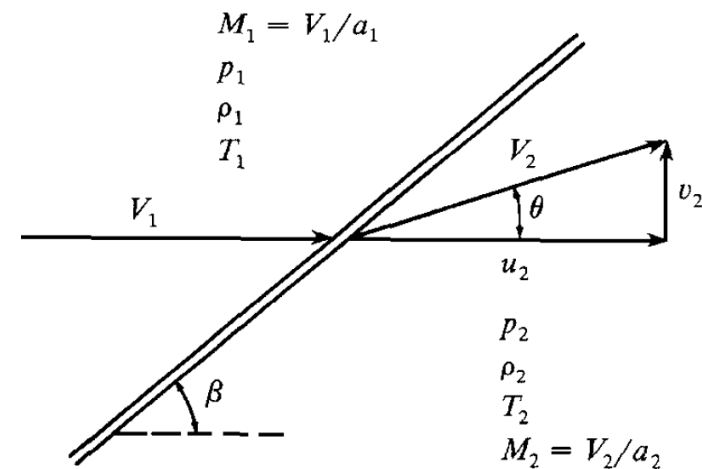
HYPERSONIC SHOCK WAVE RELATIONS

In a similar vein, the density and temperature ratios are given by

Exact:
$$\frac{\rho_2}{\rho_1} = \frac{(\gamma + 1)M_1^2 \sin^2 \beta}{(\gamma - 1)M_1^2 \sin^2 \beta + 2}$$

as $M_1 \to \infty$:
$$\boxed{\frac{\rho_2}{\rho_1} = \frac{\gamma + 1}{\gamma - 1}}$$

$$\frac{T_2}{T_1} = \frac{(p_2/p_1)}{(\rho_2/\rho_1)} \qquad \text{(from the equation of state: } p = \rho RT)$$

as $M_1 \to \infty$:
$$\boxed{\frac{T_2}{T_1} = \frac{2\gamma(\gamma - 1)}{(\gamma + 1)^2} M_1^2 \sin^2 \beta}$$

HYPERSONIC SHOCK WAVE RELATIONS

In aerodynamics, pressure distributions are usually quoted in terms of the nondimensional pressure coefficient C_p, rather than the pressure itself. The pressure coefficient is defined as

$$C_p = \frac{p_2 - p_1}{q_1}$$

where p_1 and q_1 are the upstream (free-stream) static pressure and dynamic pressure. respectively.
we obtain an exact relation for C_p behind an oblique shock wave as follows:

Exact:
$$C_p = \frac{4}{\gamma + 1}\left(\sin^2\beta - \frac{1}{M_1^2}\right)$$

as $M_1 \rightarrow \infty$:
$$\boxed{C_p = \left(\frac{4}{\gamma + 1}\right)\sin^2\beta}$$

HYPERSONIC SHOCK WAVE RELATIONS

The relationship between Mach number M_1, shock angle β, and deflection angle θ is expressed by the so-called θ-β-M relation given by Eq. (4.17), repeated below:

Exact:
$$\tan \theta = 2 \cot \beta \left[\frac{M_1^2 \sin^2 \beta - 1}{M_1^2(\gamma + \cos 2\beta) + 2} \right] \quad (15.12)$$

This relation is plotted in Fig. 4.8, which is a standard plot of wave angle versus deflection angle, with Mach number as a parameter. Returning to Fig. 4.8, we note that, in the hypersonic limit, where θ is small, β is also small. Hence, in this limit, we can insert the usual small-angle approximations into Eq. (15.12):

$$\sin \beta \approx \beta$$
$$\cos 2\beta \approx 1$$
$$\tan \theta \approx \sin \theta \approx \theta$$

resulting in

$$\theta = \frac{2}{\beta} \left[\frac{M_1^2 \beta^2 - 1}{M_1^2(\gamma + 1) + 2} \right] \quad (15.13)$$

HYPERSONIC SHOCK WAVE RELATIONS

Applying the high Mach number limit to Eq. (15.13), we have

$$\theta = \frac{2}{\beta} \left[\frac{M_1^2 \beta^2}{M_1^2 (\gamma + 1)} \right] \tag{15.14}$$

In Eq. (15.14) M_1 cancels, and we finally obtain in both the small-angle and hypersonic limits:

as $M_1 \rightarrow \infty$ and θ hence β is small:

$$\boxed{\frac{\beta}{\theta} = \frac{\gamma + 1}{2}} \tag{15.15}$$

Note that for $\gamma = 1.4$,

$$\boxed{\beta = 1.2\theta} \tag{15.16}$$

It is interesting to observe that, in the hypersonic limit for a slender wedge, the wave angle is only 20 percent larger than the wedge angle—a graphic demonstration of a thin shock layer in hypersonic flow. (Check Fig. 15.3, drawn from exact oblique shock results, and note that the 18° shock angle is 20 percent larger than the 15° wedge angle at Mach 36—truly an example of the hypersonic limit.)

NEWTONIAN THEORY

$$C_p = \frac{4}{\gamma + 1} \left[\sin^2 \beta - \frac{1}{M_\infty^2} \right] \qquad (15.10)$$

Equation (15.11) gave the limiting value of C_p as $M_\infty \to \infty$, repeated here:

as $M_\infty \to \infty$: $\qquad C_p \to \frac{4}{\gamma + 1} \sin^2 \beta \qquad (15.11)$

Now take the additional limit of $\gamma \to 1.0$. From Eq. (15.11), in both limits as $M_\infty \to \infty$ and $\gamma \to 1.0$, we have

$$C_p \to 2 \sin^2 \beta \qquad (15.17)$$

Let us go further. Consider the exact oblique shock relation for ρ/ρ_∞, given by Eq. (4.8), repeated here (again with a subscript ∞ replacing the subscript 1):

$$\frac{\rho_2}{\rho_\infty} = \frac{(\gamma + 1)M_\infty^2 \sin^2 \beta}{(\gamma - 1)M_\infty^2 \sin^2 \beta + 2} \qquad (4.8)$$

NEWTONIAN THEORY

Equation (15.2) was obtained as the limit where $M_\infty \rightarrow \infty$, namely,

as $M_\infty \rightarrow \infty$:
$$\frac{\rho_2}{\rho_\infty} \rightarrow \frac{\gamma + 1}{\gamma - 1} \qquad (15.2)$$

In the additional limit as $\gamma \rightarrow 1$, we find

as $\gamma \rightarrow 1$ and $M_\infty \rightarrow \infty$:
$$\boxed{\frac{\rho_2}{\rho_\infty} \rightarrow \infty} \qquad (15.18)$$

i.e., the density behind the shock is infinitely large. In turn, mass flow considerations then dictate that the shock wave is coincident with the body surface. This is further substantiated by Eq. (15.15), which is good for $M_\infty \rightarrow \infty$ and small deflection angles

$$\frac{\beta}{\theta} \rightarrow \frac{\gamma + 1}{2} \qquad (15.15)$$

In the additional limit as $\gamma \rightarrow 1$, we have:

as $\gamma \rightarrow 1$ and $M_\infty \rightarrow \infty$ and θ and β small:

$$\boxed{\beta = \theta}$$

i.e., the shock wave lies on the body. In light of this result, Eq. (15.17) is written as

$$\boxed{C_p = 2 \sin^2 \theta} \qquad (15.19)$$

NEWTONIAN THEORY

In the newtonian model of fluid flow, the particles in the free stream impact only on the frontal area of the body; they cannot curl around the body and impact on the back surface. Hence, for that portion of a body which is in the "shadow" of the incident flow, such as the shaded region sketched in Figures no impact pressure is felt.
Hence, over this shadow region it is consistent to assume that $p = p_\infty$, and therefore $C_p = 0$, as indicated in Figures:
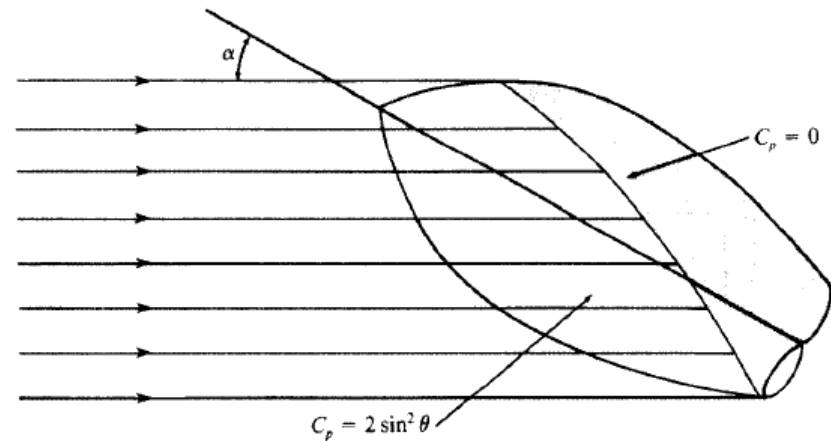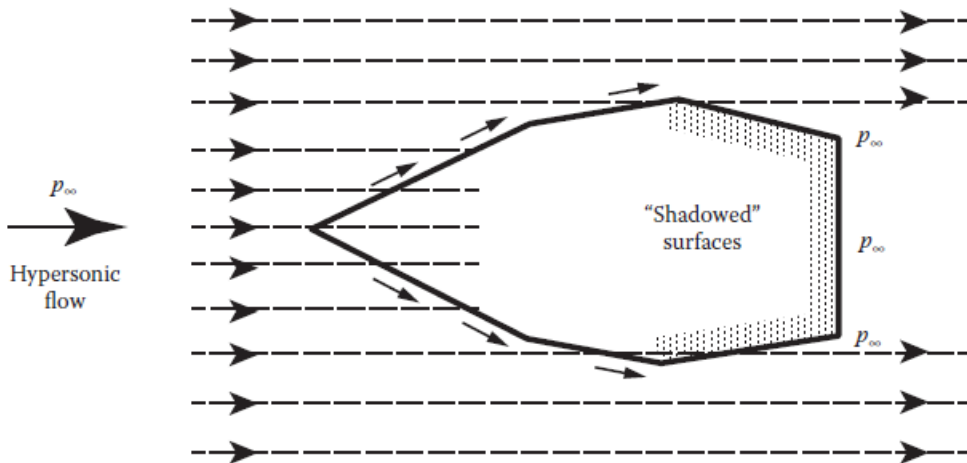
NEWTONIAN THEORY

In It is instructive to examine newtonian theory applied to a flat plate, as sketched in Fig. Here, a two-dimensional flat plate with chord length c is at an angle of attack a to the free stream. Since we are not including friction, and because surface pressure always acts normal to the surface, the resultant aerodynamic force is perpendicular to the plate, i.e., in this case the normal force N is the resultant aerodynamic force. In turn, N is resolved into lift and drag, denoted by L and D, respectively, as shown in Fig. According to

newtonian theory, the pressure coefficient on the lower surface is

$$C_{p_l} = 2 \sin^2 \alpha$$

and that on the upper surface, which is in the shadow region, is

$$C_{p_u} = 0$$

NEWTONIAN THEORY

Defining the normal force coefficient as $c_n = N/q_\infty S$, where $S = (c)(l)$, we can readily calculate c_n by integrating the pressure coefficients over the lower and upper surfaces (see, for example, the derivation given in Ref. 104):

$$c_n = \frac{1}{c} \int_0^c \left(C_{p_l} - C_{p_u} \right) dx \qquad (15.22)$$

where x is the distance along the chord from the leading edge. Substituting Eqs. (15.20) and (15.21) into (15.22), we obtain

$$c_n = \frac{1}{c}(2 \sin^2 \alpha)c$$

or
$$c_n = 2 \sin^2 \alpha \qquad (15.23)$$

From the geometry of Fig. 15.10, we see that the lift and drag coefficients, defined as $c_l = L/q_\infty S$ and $c_d = D/q_\infty S$, respectively, where $S = (c)(l)$, are given by

$$c_l = c_n \cos \alpha \qquad (15.24)$$

and
$$c_d = c_n \sin \alpha \qquad (15.25)$$